# Self-Propagating High-Temperature Synthesis of Chromium Substituted Lanthanide – Barium – Copper Oxides, $LnBa_2Cu_{3-x}Cr_xO_{7-y}$ (Ln = Y; La; Nd; Sm and Yb)

Maxim V. Kuznetsov[1*], Ivan P. Parkin[2], Yuri G. Morozov[1] and Alexander G. Merzhanov[1]

[1]Institute of Structural Macrokinetics and Materials Science Russian Academy of Sciences, p/o Chernogolovka, Moscow Region, 142432 Russia

[2]Department of Chemistry, Christopher Ingold Laboratory, University College London, 20 Gordon Street, London, WC1H 0AJ UK

## Abstract

A series of $MBa_2Cu_{3-x}Cr_xO_{7-y}$ (M = Y; La; Nd; Sm and Yb; $x$ = 0, 0.05, 0.15, 0.25) materials were synthesized in air by self-propagating high-temperature synthesis (SHS) involving reaction of stoichiometric mixtures of rare-earth metal (III) oxide, barium peroxide, copper metal, chromium (III) oxide and sodium perchlorate. All the SHS processes were followed by sintering in oxygen at 950°C for 2h. The products were characterized by SEM, X-ray powder diffraction, UV, superconductive transition temperatures ($T_c$) and magnetic susceptibility ($\chi$) measurements. X-ray diffraction data showed that single phase orthorhombic (or tetragonal for M = Nd) materials were produced. All series of materials showed a systematic increase in lattice parameters and unit cell volume with chromium content (M = Y: $x$ = 0, $V$ = 174.25 Å$^3$; $x$ = 0.25, $V$ = 175.10 Å$^3$). Thermal stability of all the SHS prepared materials increased with $x$. Oxygen content of all the samples increased with $x$, but did not exceed 7.0. Superconductivity transition temperature decreased with chromium substitution in all systems (98-77 K). Magnetic susceptibility decreased with chromium substitution.

## Introduction

High temperature superconducting materials (HTSC) such as $LnBa_2Cu_3O_{7-y}$ (Ln = Y or rare-earth metal (REM)) are of widespread engineering, academic and industrial interest. The amount and distribution of dopants into the classic 1-2-3 host material $LnBa_2Cu_3O_{7-y}$ has been important in deriving improvements in $T_c$ and in developing an understanding of superconductivity [1]. In this connection, it is necessary to gain information about doped materials with homogeneous or inhomogeneous dopant distributions. Such materials are important for finding out the method of entry and position of the dopant within the crystal structure. Such studies enable an understanding of the influence of dopant on superconducting properties. Materials with known dopant distributions can be used for the creation of crystalline heterostructures such as HTSC - metal or HTSC - dielectrics that can be used for industrial purposes. Chromium doping into $LnBa_2Cu_3O_{7-y}$ moderately reduces the $T_c$ by replacement of one of the cations to promote formation of $Ln_{1-x}Cr_xBa_2Cu_3O_{7-d}$; $LnBa_{2-x}Cr_xCu_3O_{7-d}$ or $LnBa_2Cu_{3-x}Cr_xO_{7-d}$.

High temperature superconducting materials have been made by SHS, Eqn. 1.

$$3Cu + 2BaO_2 + 0.5Y_2O_3 + 0.75O_2 \rightarrow YBa_2Cu_3O_{7-x} \quad (1)$$

In this process copper gets oxidized and provides the fuel for the reaction; $BaO_2$ is a solid oxidizer and $Y_2O_3$ – an active dilutient [2]. The reaction is rapid producing HTSC materials in seconds from the exothermic oxidation of copper metal. The mechanism of this reaction has been established by a series of detailed thermodynamic measurements.

*corresponding authors. E-mail: kvin@kuznetsov.home.chg.ru

Formation of the SHS product in the system Cu + $BaO_2$ + $O_2$ occurs in two ways:

$$Cu + O_2 \rightarrow Cu_2O \cdot CuO \qquad (2)$$

and

$$Cu + BaO_2 \rightarrow BaCuO_2 \qquad (3)$$

The initial stages involve the oxidation of copper by gaseous oxygen Eqn. 2, this produces sufficient energy to promote Eqn. 3 where $BaO_2$ gets involved in the process.

The simplified reaction scheme for the chemistry involved in preparation of 1-2-3 HTSC materials by SHS is shown in Eqn. 4 and Eqn. 5.

$$3Cu + 2BaO_2 + 0.5Y_2O_3 + O_2 \rightarrow Ba_2Cu_3O_5 + 0.5Y_2O_3 + O_2 \rightarrow YBa_2Cu_3O_{7-x} \qquad (4)$$

$$3Cu + 2BaO_2 + 0.5Y_2O_3 \rightarrow 2BaCuO_2 + Cu + 0.5Y_2O_3 \rightarrow 0.5Y_2BaCuO_5 + Cu + 1.5\ BaCuO_2 \qquad (5)$$

The route shown in Eqn. 2 is realized when sufficient gaseous oxygen reaches the reaction zone, and the route shown in Eqn. 3 – with an oxygen deficiency. Thus, during the SHS combustion an active melt is formed that contains BaO and occurs on the surface of copper particles. Copper is partially oxidized by oxygen from the melt, and the oxygen deficiency for the whole reaction is compensated for by absorption from the atmosphere. The final $Y_{123}$ product was formed in the SHS step by crystallization of a melt of $Y_2O_3$, barium cuprates and copper (II) oxide. This produces fine crystals of $YBa_2Cu_3O_{7-y}$.

During the SHS of $YBa_2Cu_3O_4$, $BaCuO_2$ and $BaCu_2O_2$ intermediates were formed. The formation of $BaCu_2O_2$ is a distinctive characteristic of the SHS process in comparison with standard ceramic technology. Its formation is connected to the oxygen deficit caused by the decomposition of $BaO_2$ being faster than the copper oxidation. In mixed melts of the $BaCuO_2$ - $BaCu_2O_2$ materials and $Y_2O_3$ readily dissolve, this together with the cuprates CuO already presented in the melt, results in a number of cases results to the reaction:

$$BaCuO_2 + CuO \rightarrow BaCu_2O_2 + 0.5O_2\uparrow \qquad (6)$$

In parallel with that reaction in the cuprate melt the following reaction also proceeds:

$$Y_2O_3 + BaCu_2O_2 + CuO \rightarrow Y_{123} \qquad (7)$$

The reaction shown in Eqn. 6 provides a continuous source of $BaCu_2O_2$ in the reaction zone, and oxygen. Oxygen filtration from the external environment is carried out by chemical means of formation of intermediate phases: $BaCu_2O_2 + O_2 \rightarrow BaCuO_2 + CuO + O_2\uparrow \rightarrow BaCuO_{2.5} + CuO + O_2\downarrow \rightarrow BaCuO_2 + CuO + O_2\downarrow \rightarrow BaCu_2O_2$ [3].

The experimental procedure for conventional synthesis of chromium substituted HTSC involves long firing times with intermediate grinding operations. Den et al. [4] took high purity starting materials (> 99.9%) $Y_2O_3$, $SrCO_3$, CuO and $Cr_2O_3$ which were weighed out in the appropriate molar proportions and mixed through grinding in a mechanical mortar and pestle for 1h. After an initial reaction at 1040-1060°C in alumina crucibles, samples were reground, pressed into pellets and heated in an $O_2$ flow for 2 h at the same temperature. Andresen et al. [5] prepared Cr-substituted $Y_{123}$ by multiple firing of precursors obtained by liquid mixing in citrate gels; $Y_2O_3$, $BaCO_3$, $CuCO_3 \cdot Cu(OH)_2 \cdot 0.5H_2O$ were dissolved in boiling citric acid mono hydrate and $CrO_3$ added in a water soluble form. The gel that formed was dried at 180°C, incinerated in air, milled, pelletized and fired at 910°C for 20 h in a corundum boat under flowing oxygen, before being finally oxidized at 340°C for 16 h. The firing procedure was repeated twice. The above methods have multiple step pathways that are time consuming and expensive. In this paper we report an inexpensive, two step route for the preparation of Cr-substituted HTSC $Ln_{123}$ – type via SHS reactions. In particular we report on the reaction pathway in the SHS processes by a series of thermal measurements and compare the $T_c$ and magnetic properties of the products to conventionally made materials.

## Experimental

All reagents were obtained from Aldrich Chemical Co. (UK) and used as supplied. All the manipulations and weightings were carried out under nitrogen atmosphere in a Saffron Glove Box (Saffron Scientific Equipment Ltd). Milling operations were carried out in a FRITSCH 05.102 ball mill using Halcedon containers and balls. All the SHS reactions were carried out in air with pressed cylindrical samples

(diameter = 20 mm; height = 40 mm). Ignition operations were made by REKROW (RK-2060). Combustion temperatures were measured using tungsten-rhenium (5% and 20% Re) thermocouples. Sintering was carried out in a quartz tube (*i.d.* 80 mm) under a flow of oxygen on reground powders using a Nabertherm programmable tube furnace. Heating and cooling rates were 10°C/min. X-ray powder diffraction was performed in the reflection mode on a Philips X-pert diffractometer using unfiltered $CuK_\alpha$ radiation ($\lambda_1$ = 1.5405 Å, $\lambda_2$ = 1.5443 Å). Phases were identified and indexed using the JCPDS database, ASTM and Unit Cell programs. Pycknometrical densities were measured by standard methods using toluene; magnetic and superconducting characteristics were investigated using EG&G PARC 4500 at room and liquid nitrogen temperatures; TGA and DTA experiments were carried out on SETARAM TAG24 using alumina standards with heating and cooling rates of 10°C/min. SEM/EDAX were determined on a Hitachi S300 and JEOL EMA instruments. UV spectra were obtained on a Shimadzu UV-2041 using pressed KBr disks (sample:KBr ratio is 1:20). The oxygen content was determined iodomerically. The accuracy of determination is ± 0.01.

SHS reactions were performed on various starting mixtures of appropriate REM (III) oxide $Ln_2O_3$, $BaO_2$, Cu, $Cr_2O_3$ and $NaClO_4$. The molar ratio of an each reagent was chosen to conform to the stoichiometry and oxygen content (7.0) of the product. Sodium perchlorate, as well as barium peroxide was used as an internal oxidising agent for the combustion processes. On decomposition, these compounds produce oxygen which oxidises the Cu metal - the fuel source of the reaction. Sodium chloride is also produced on decomposition of the perchlorate. This provides additional energy for the reaction and acts as a wetting agent that helps to ensure passage of the propagation wave through the solid. The sodium chloride is partially evaporated during the SHS process, the remainder is readily removed from the product by washing with $CCl_4$. The general reaction scheme for the formation of Cr-doped 1-2-3 HTSC formed by SHS was:

$$0.5\ Ln_2O_3 + 2BaO_2 + (3\text{-}x)\ Cu + 0.5xCr_2O_3 + \\ + (1.5\text{-}3x)/4\ NaClO_4 \rightarrow LnBa_2Cu_{3-x}Cr_xO_{7-y} + \\ + (1.5\text{-}3x)/4\ NaCl \qquad (8)$$

where x = 0-0.25, Ln = Y; Nd; Sm; Yb; La

The critical concentration of sodium perchlorate, when the process was not conducted in air is ~ 0.2 molar equivalents. This ensures that sufficient oxygen is available for the reaction. The formation of copper oxide slows down the SHS combustion reaction, similar to conventional synthesis, as the copper oxide tends to coat the copper metal particles and shields the surface from further oxidation. Using an internal oxidizer such as barium oxide or sodium perchlorate helps to alleviate this problem, especially with regard to oxygen diffusion from the atmosphere. The initial SHS reaction produces $LnBa_2Cu_{3-x}Cr_xO_7$ contaminated with NaCl and a few other minor phases associated with incomplete combustion. To improve the materials purity the as formed solid were washed with $CCl_4$ and then annealed at 950°C for 2 h.

It is necessary to note, that Cr insertion in the reaction mixture was obtained in two ways, by conventional SHS as detailed above and by mixing an appropriate quantity of chromium (III) oxide with pre made $Y_{123}$. This later mixture was pressed into pellets and annealed for some hours in a flowing oxygen.

### *Preparation of $LnBa_2Cu_{2.75}Cr_{0.25}O_{7-y}$ from reaction of $Nd_2O_3$; $BaO_2$; Cu; $Cr_2O_3$ and $NaClO_4$. Ln = La; Y; Nd; Sm and Yb.*

The same reaction scale and procedure was adopted for all the lanthanides illustrated here for Ln = Nd. $Nd_2O_3$ (4.80 g), barium peroxide (9.66 g), chromium (III) oxide (0.54 g), copper metal (5.00 g) and sodium perchlorate (0.94 g) were ground for 1 h in a ball mill using Halcedon boxes and balls (balls: green mixture ratio is 10:1). The mixture was pressed (20 kg/cm$^2$) into a 2 cm by *ca.* 4 cm cylindrical pellet. Small holes were drilled through pellet and W-Re thermocouples inserted. The pellet was supported on a ceramic plate and the reaction ignited by a micro torch (ignition temperature is ~ 1200°C) at the top. This produced a light orange propagation wave that proceeded through the solid at *ca.* 1-2 mm/s. The average reaction temperature was 900-930°C. This produced a black solid which was ground in a pestle and mortar, washed with $CCl_4$ (3×200 ml) filtered through a Buchner funnel and placed on the quartz boat inside of the Nabertherm furnace. Samples were annealed in flowing oxygen at a temperature of 950°C for 2h. Yields were essentially quantitative. The solid was analyzed by X-ray powder diffraction. The resultant black powder was tetragonal (*a* = 5.517 Å; *c* = 7.719 Å) with single phase $Nd_{123}$. Tran-

sition temperature and magnetic susceptibility for all the samples were also measured (Tables 1 and 2). EDAX showed consistent Nd:Ba:Cu (1:2:2.75) ratios across all surface spots.

**Table 1**

Lattice parameters for the five series of $MBa_2Cu_{3-x}Cr_xO_{7-y}$ (M = Y; La; Nd; Sm; Yb) HTSC samples obtained following the SHS reaction of $BaO_2$, Cu, $M_2O_3$, $Cr_2O_3$ and $NaClO_4$. In all the cases samples was sintered in flowing oxygen at 950°C for 2 h after the initial SHS. The lattice parameters, unit cell volumes *V* (Å), *a/b* and *b/c* orthorhombicity parameters, X-ray ($d_x$, g/cm$^3$) and pycnometric ($d_{pycn}$, g/cm$^3$) densities, obtained at room temperature, were also listed below.

| M | x | *a*/Å (± 0.002) | *b*/Å (± 0.002) | *c*/Å (± 0.005) | *a*/*b* | *c*/*b* | *V*/Å$^3$ (± 0.5) | d |
|---|---|---|---|---|---|---|---|---|
| Y | 0* | 3.818 | 3.901 | 11.649 | 0.979 | 2.986 | 173.50 | - |
| | 0** | 3.824 | 3.896 | 11.655 | 0.982 | 2.992 | 173.64 | $6.10_p$ |
| | 0*** | 3.824 | 3.888 | 11.650 | 0.984 | 2.996 | 172.21 | $6.34_x$ |
| | 0 | 3.828 | 3.899 | 11.675 | 0.982 | 2.994 | 174.25 | $5.02_p$ |
| | 0.05 | 3.829 | 3.900 | 11.676 | 0.982 | 2.994 | 174.36 | $5.21_p$ |
| | 0.15 | 3.833 | 3.908 | 11.678 | 0.981 | 2.988 | 174.93 | $5.30_p$ |
| | 0.25 | 3.835 | 3.908 | 11.683 | 0.981 | 2.990 | 175.10 | $5.42_p$ |
| La | 0*** | 3.907 | 3.920 | 11.798 | 0,997 | 3.010 | 180.69 | $6.95_x$ |
| | 0 | 3.912 | 3.910 | 11.733 | 1.001 | 3.001 | 179.47 | $5.20_p$ |
| | 0.05 | 3.915 | 3.912 | 11.736 | 1.001 | 3.000 | 179.74 | $5.30_p$ |
| | 0.15 | 3.920 | 3.916 | 11.740 | 1.001 | 3.000 | 180.22 | $5.40_p$ |
| | 0.25 | 3.921 | 3.917 | 11.756 | 1.001 | 3.000 | 180.51 | $5.69_p$ |
| Sm | 0*** | 3.902 | 3.844 | 11.725 | 1.015 | 3.050 | 175.87 | $6.87_x$ |
| | 0 | 3.891 | 3.841 | 11.725 | 1.013 | 3.053 | 175.23 | - |
| | 0.05 | 3.907 | 3.847 | 11.732 | 1.016 | 3.050 | 175.33 | - |
| | 0.15 | 3.911 | 3.849 | 11.740 | 1.016 | 3.050 | 176.73 | - |
| | 0.25 | 3.912 | 3.850 | 11.748 | 1.016 | 3.051 | 176.94 | - |
| Yb | 0*** | 3.871 | 3.802 | 11.658 | 1.018 | 3.012 | 171.58 | $7.26_x$ |
| | 0 | 3.857 | 3.790 | 11.671 | 1.018 | 3.079 | 170.61 | $5.80_p$ |
| | 0.05 | 3.864 | 3.799 | 11.675 | 1.017 | 3.073 | 171.38 | $5.90_p$ |
| | 0.15 | 3.866 | 3.803 | 11.684 | 1.017 | 3.072 | 171.78 | $6.10_p$ |
| | 0.25 | 3.868 | 3.808 | 11.693 | 1.016 | 3.071 | 172.23 | $6.22_p$ |
| Nd | 0*** | 5.520 | 5.520 | 11.709 | 1.000 | 2.121 | 356.78 | - |
| | 0 | 5.505 | 5.505 | 11.710 | 1.000 | 2.127 | 354.87 | $5.70_p$ |
| | 0.05 | 5.508 | 5.508 | 11.716 | 1.000 | 2.127 | 355.44 | $5.75_p$ |
| | 0.15 | 5.513 | 5.513 | 11.718 | 1.000 | 2.126 | 356.15 | $5.80_p$ |
| | 0.25 | 5.517 | 5.517 | 11.719 | 1.000 | 2.124 | 356.69 | $5.90_p$ |

* - Industrial product of Aldrich Chem. Co. (UK), 35,746-4 [107539-20-8]

** - SHS in an atmosphere of oxygen ($PO_2$ = 1 atm)

*** - Reference samples (JSPDC - International Center for Diffraction Data)

**Table 2**

Transition temperature ($T_c$, K) of SHS products $LnBa_2Cu_{3-x}Cr_xO_{7-y}$ (Ln = Y; Nd; Sm; Eu; Gd; Dy; Ho; Yb; Lu) sintered in the flowing oxygen at 950°C for 2h and magnetic susceptibility ($\chi \bullet 10^{-6}$, $cm^3/g$) of HTSC materials at room temperature and oxygen content (7-y).

| Synthesis procedure | | Ln (rare-earth metal) | | | | | | | | |
|---|---|---|---|---|---|---|---|---|---|---|
| | | Y | Nd | Sm | Eu | Gd | Dy | Ho | Yb | Lu |
| SHS in oxygen atmosphere ($PO_2$ = 1 atm) [9] $T_c$ at x = 0 | | 93 | 85 | 94 | 98 | 99 | 97 | 96 | 94 | 98 |
| SHS with solid oxidizer ($NaClO_4$) $T_c$ at: | | | | | | | | | | |
| x = 0 | $T_c$ | 91 (6.65) | 84 | 93 (6.70) | 96 | 98 | 97 | 96 | 94 | 97 |
| | $\chi$ | 23.1 | 65.1 | 32.0 | - | - | - | - | 96.6 | - |
| x = 0.05 | $T_c$ | 90 | 80 | 90 | - | - | - | - | 91 | - |
| | $\chi$ | 18.3 | 62.7 | 25.5 | - | - | - | - | 94.9 | - |
| x = 0.15 | $T_c$ | 88 (6.71) | 77 | 85 (6.77) | - | - | - | - | 88 | - |
| | $\chi$ | 17.6 | 61.9 | 24.5 | - | - | - | - | 92.7 | - |
| x = 0.25 | $T_c$ | 86 (6.75) | - | 82 (6.81) | - | - | - | - | 85 | - |
| | $\chi$ | 16.8 | 60.1 | 22.4 | - | - | - | - | 91.0 | - |

## Results and discussions

### *SHS product characterisation*

All the SHS products were dense lightly melted black agglomerates, that were fragile and broke under manipulation. The average granulometric size of the as-synthesis products is $d_{av}$ ~ 20-24 microns. Unfortunately, commercially available rare-earth metal powders, were not suitable as a fuel for the SHS reactions. For example, the minimal particle size of all the REM metal powders from Aldrich Chem.Co. (UK) is ~ 425 microns, whereas the limiting particle size of powders, at which use is possible to produce the HTSC product in combustion reactions is 60-80 microns. For such powders to be used in SHS requires additional milling and other treatment in special high-hardness ball mills and attritors.

The major product in the SHS reactions was the $YBa_2Cu_{3-x}Cr_xO_{7-y}$ product, however impurities such as $Y_{211}$ (green phase), barium cuprate $BaCuO_2$ and CuO were also observed (*ca* 10-20%). A short annealing step of this composite powder in flowing oxygen at T = 950°C for 2 h removed the impurities and formed single phase $YBa_2Cu_{3-x}Cr_xO_{7-y}$ (Fig. 1). The formation of impurities is related to the small samples size and incomplete combustion which leads to nonequilibrium product formation. This is related to the short synthesis and cooling times involved in SHS. Additional heat treatment promotes an increase of uniformity, mainly in terms of oxygen content and promotes greater crystallization. An annealing temperature of 950°C was noted as optimum. It was found that annealing temperatures greater than 1100°C lead to product degradation and formation of $Y_2BaCuO_5$ and CuO. At the highest level of $Cr_2O_3$ used a trace of copper (II) oxide and chromium (III) oxide were also found in the final product even after the supplementary annealing in oxygen (*ca* < 1%).

Copper is distributed in the $Ln_{123}$ material between two non equivalent crystallographic positions, $Cu^{2+}$ and $Cu^{3+}$. Introducing chromium into the $Ln_{123}$ structure increase the orthorhombic cell parameters *a, b* and *c*. The substitutional behavior of copper sites are not identical, and increasing of the orthorhombic parameters may be explaining clearly by the occupation of $Cu^{3+}$ sites by $Cr^{3+}$ atoms ($Cr^{3+}$ (0.755 Å) has a higher ionic radius than copper $Cu^{3+}$ (0.680 Å) but lower than $Cu^{2+}$ (0.870 Å)). Inside of each series of $LnBa_2Cu_{3-x}Cr_xO_{7-y}$ (Ln = Y; La; Nd; Sm and Yb) the degree of orthorhombicity of the elementary cell *a/b* and *c/b* for all *x* (Table 1) were practically the same. An increase of the Ln ionic radii is related to the degree of orthorhombicity *a/b* and *c/b* that was noted to

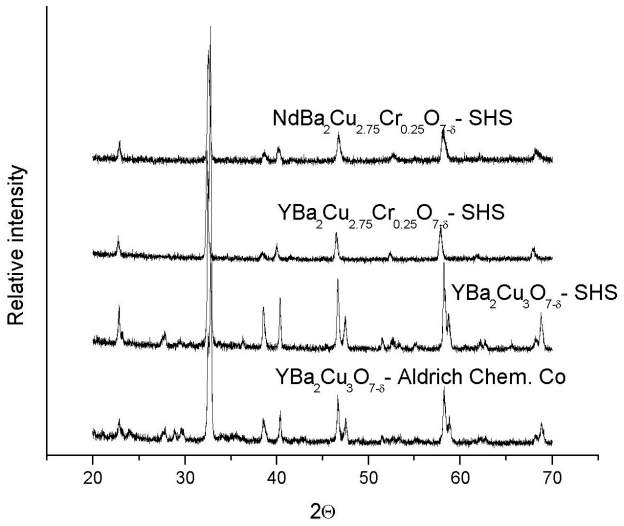


Fig.1. XRD pattern of reference $YBa_2Cu_3O_{7-y}$ pattern (Aldrich Chem.Co (UK)); SHS prepared $YBa_2Cu_3O_{7-y}$, $YBa_2Cu_{2.75}Cr_{0.25}O_{7-y}$ and $NdBa_2Cu_{2.75}Cr_{0.25}O_{7-y}$.

increase from 0.982 and 2.994 for yttrium up to 1.018 and 3.079 for ytterbium. Inside of each system with increasing *x* the parameter *(b-x)* changes with a maximum at 0.012. All the Nd-containing compounds have a tetragonal structure. For this series the *a* and *c* values also increase with *x*. The *c/b* parameter however is practically identical for all degrees of chromium substitution into $NdBa_2Cu_{3-x}Cr_xO_{7-y}$. Substitution is one of the most effective methods to influence the material's density (Table 1). In all the systems investigated pycknometric density of the SHS products increased with chromium content. Such doping is supposed to be effective in optimizing the properties of $Ln_{123}$ superconductors for practical applications.

EDAX elemental analysis of the SHS products indicates high uniformity with no phase segregation. The IR spectra of HTSC materials in a range of 50-4000 $cm^{-1}$ show no evidence for formation of a secondary $Cr_2O_3$ phase. The UV-spectra of undoped and chromium-substituted samples reveal virtually no changes in absorption with Cr content.

An increase in chromium substitution in the SHS prepared materials results in products with higher thermal stability. Comparison of undoped and chromium-substituted products allows the following conclusions: an orthorhombic $YBa_2Cu_3O_{7-y}$ sample heated in the temperature range of 400-850°C leads to a ~ 0.8% mass (Fig. 2a) reduction. This is allocated to loss of coordinated water. At higher temperatures degradation of the superconducting phase occurs, this phase transition takes place with maximum thermal evolution observed at T = 940°C. However, the orthorhombic HTSC $YBa_2Cu_3O_{7-y}$ phases have a reversible characteristics, this is shown by the presence of exothermic peaks on the cooling curve and is accompanied by the restoration of superconducting properties at the end of the process. Heating the chromium-substituted sample $YBa_2Cu_{2.75}Cr_{0.25}O_{7-y}$ shows flat thermal characteristics in the range 20-1000°C (Fig. 2b). At the same time some water loss takes place at low temperatures (T < 200°C). On the DTA curve small additional endo- and exothermic peaks are observed which are possibly related to the oxygen sorption-desorption from the HTSC structure [6]. Due to much more complex chemical composition of substituted material, large amounts of site defects are present in its anion sublattice, related to the presence of not only Cu-O, but also Cr-O bonds. At the same time, the presence of chromium and oxygen bonds have a stabilizing influence on the materials structure. In connection with this, the degradation processes in the substituted material occurs at higher temperatures and requires more heating to degrade the material. So, the convertible phase transition in the chromium substituted $Y_{123}$ (x = 0.25) takes place at T = 955°C in comparison with T = 940°C for the non-doped material.

Thermal stability of HTSC materials increased not only in the systems that have the orthorhombic elementary cells parameters, but also in the tetragonal samples $NdBa_2Cu_{3-x}Cr_xO_{7-y}$ (Figs. 2c-2d). In HTSC materials there are two types of tetragonal structures - so-called tetra (I) and tetra (II) [7]. The tetragonal product from the SHS reaction is superconducting, and its structure belongs to a tetra (I) type. In this case, during linear heating of the SHS products, the endothermic peaks in the DTA curves may be attributed to the transitions from the superconducting tetra (I) structure to the non-superconducting tetra (II) form. With an increase of chromium substitution from $x = 0$ to 0.25, the phase transition temperature was also noted to increase from 938°C to 957°C. It is necessary to note, that the tetragonal HTSC phase is characterized by lower oxygen contents in comparison with the orthorhombic one. At the same time, the *c/b* parameter is also practically identical for all values of *x*.

The ionic radii, electron affinity and orbital structure of 3d-elements and in particular chromium and copper (Cu - 1.8 eV, Cr - 1.6 eV) are similar. Related to this, it is likely, that chromium will replace Cu in the 1-2-3 structure. A suppression in $T_c$ in all the sys-

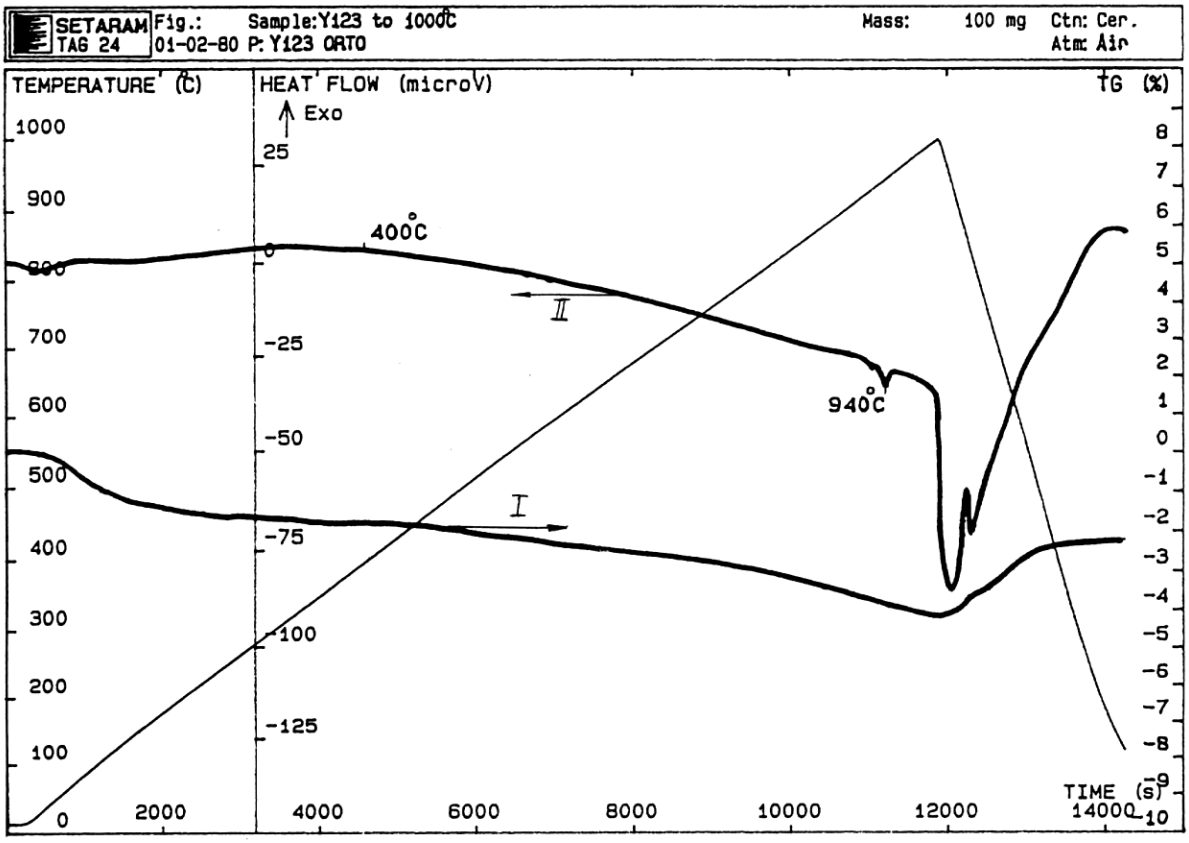


Fig. 2a. TGA (I) and DTA (II) curves for the linear heating of $YBa_2Cu_3O_{7-y}$ ($x$ = 0; orthorhombic phase).

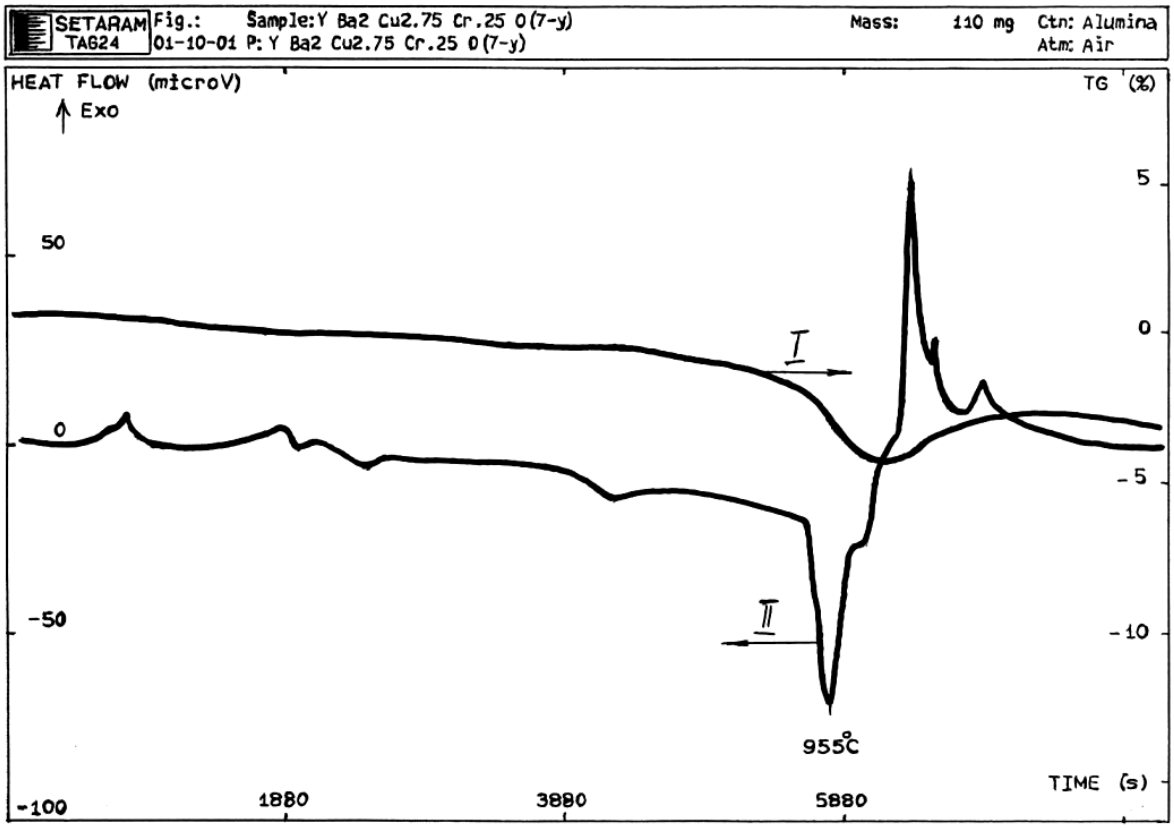


Fig. 2b. TGA (I) and DTA (II) curves for the linear heating of $YBa_2Cu_{2.75}Cr_{0.25}O_{7-y}$ ($x$ = 0.25; orthorhombic phase).

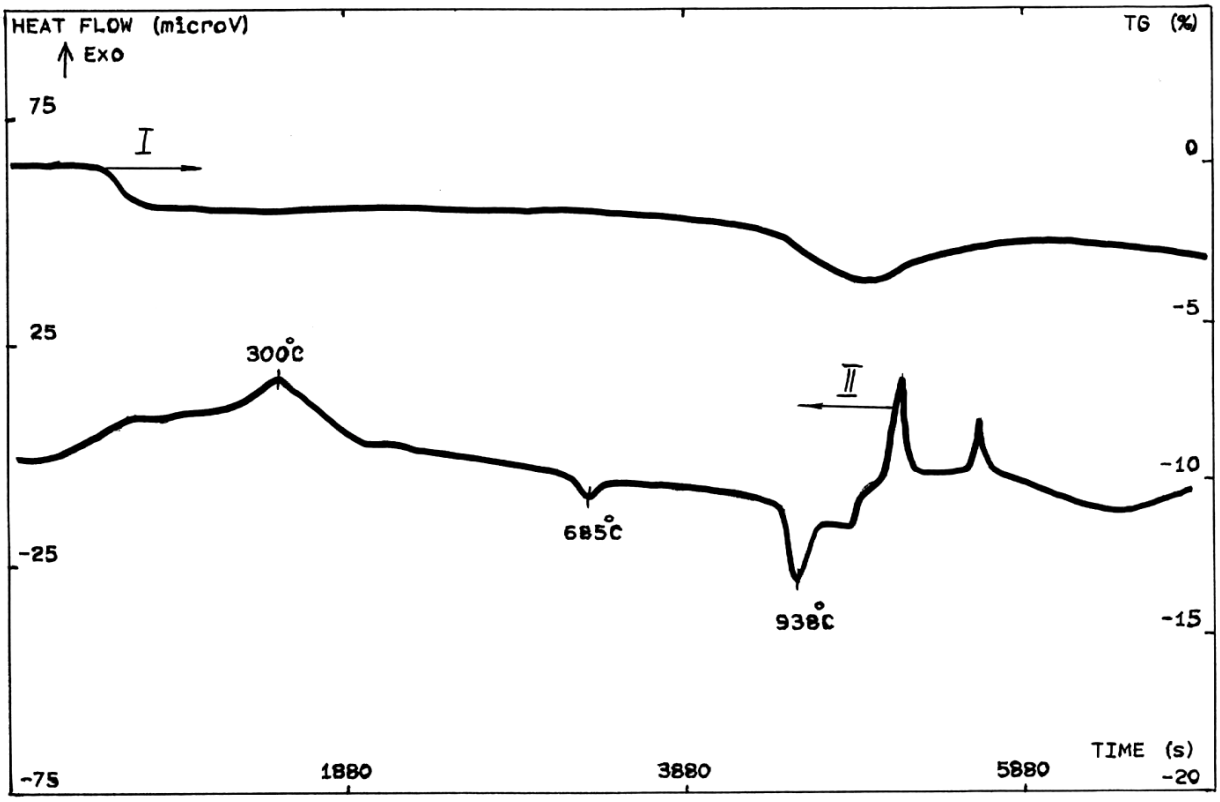


Fig. 2c. TGA (I) and DTA (II) curves for the linear heating of $NdBa_2Cu_3O_{7-y}$ ($x$ = 0; tetragonal phase).

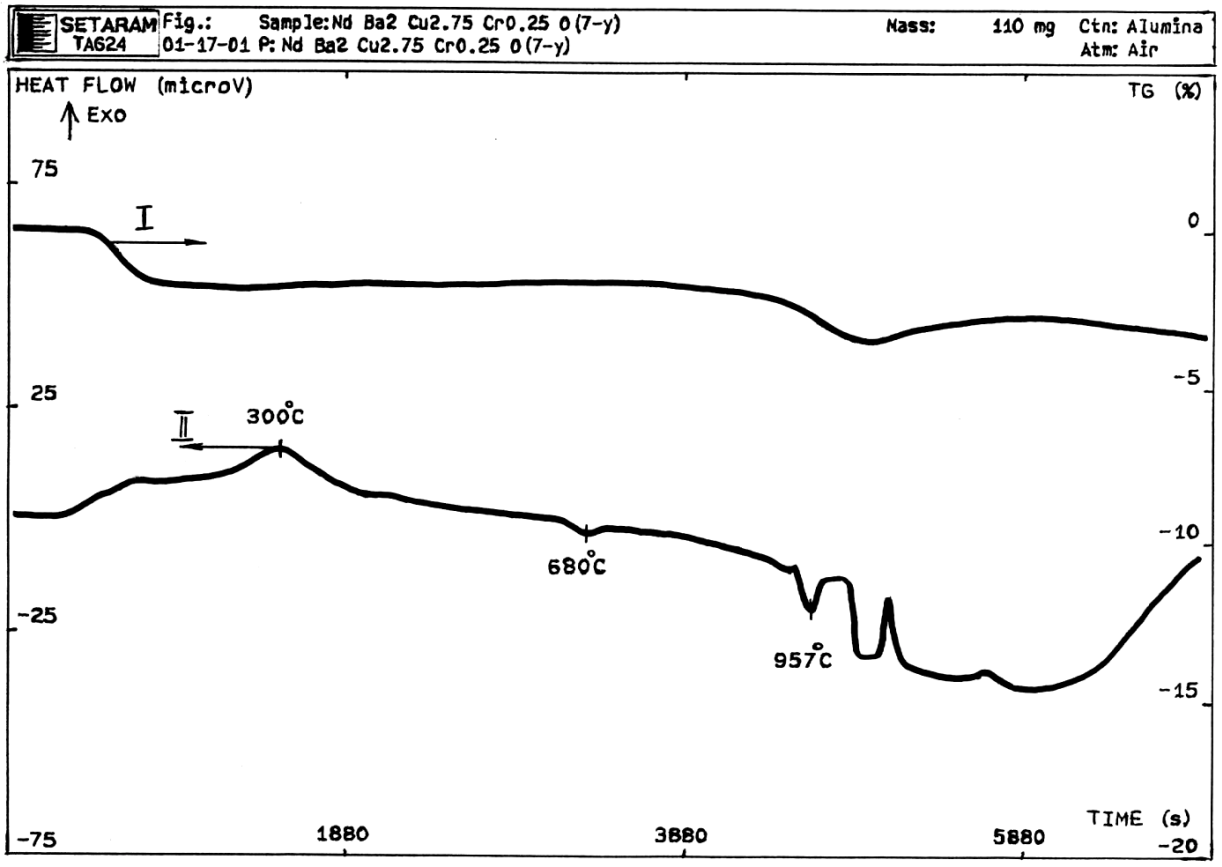


Fig. 2d. TGA (I) and DTA (II) curves for the linear heating of $NdBa_2Cu_{2.75}Cr_{0.25}O_{7-y}$ ($x$ = 0.25; tetragonal phase).

tems was observed with increasing chromium content. This is in agreement with the classical Abrikosov-Gorkov theory [8], which indicates that the magnetic moment of some dopants such as chromium (Table 2), can form specific magnetic clusters. Thus, the exchange interaction between Cooper pairs and the local magnetic moment is reduced resulting in partial suppression of superconductivity. This leads to a uniform reduction of $T_c$ with Cr content. Since superconductivity depends on carrying a charge in Cu-O (1) chains to $CuO_2$ layers, the copper replacement in the 1-2-3 structures by $Cr^{3+}$ cations influences the products oxygen stoichiometry and results in the oxygen vacancies ordering within the structure [9-14]. Oxygen content in chromium-substituted HTSC is one of the most debatable issues in a number of physico-chemical properties of this class of materials. In this connection, it is necessary to emphasize that HTSC materials such as $Y_{123}$, which were synthesized by solid-oxidizers were characterized essentially by lower oxygen contents in comparison with materials of the same chemical composition produced in an oxygen atmosphere. So, the oxygen content of non doped SHS product $YBa_2Cu_3O_{7-y}$ – synthesized by using $NaClO_4$ makes it 6.65 per formula unit, as against ~ 6.85 – for the synthesis in an oxygen atmosphere without a solid oxidiser. At the same time, the tendency of oxygen content to increase with *x* also exists in the SHS-made materials and is in agreement with results produced in [11]. The calculated oxygen content value is 7.0, but experimentally produced value at maximal x = 0.25 is 6.75. In the samarium samples in a range x = 0-0.25 values grow from 6.70 (Table 2). In a number of papers the question of oxygen concentration with doping content were discussed [10,15-16]. In accordance with [15], at *x* = 0.291 the synthesis product has rhombic cell parameters, a transition temperature of $T_c$ = 86 K and an oxygen content of 7.3. The large oxygen content in the synthesized ceramics is abnormal and was explained from the point of view of entry of impurity cation in the copper position Cu1, which was accompanied, probably, by oxygen addition in a partially vacant position O1. Umardevi and Ramamohan [11] reported it was a favorable factor for the stabilization of rhombic structure in HTSC and the preservation of superconductivity. They also reported the oxygen content (7-y) also increased with chromium content, however, the maximum value did not exceed 6.94. Thus, by using SHS products it indicates that copper replacement in the structures of the $Ln_{123}$ – type by cations with valence greater than +2 enables an ordering in the structure of oxygen vacancies of the HTSC material structure. It is also necessary to emphasize that the SHS HTSC ceramics are stable to oxygen loss. Oxygen content of both non-doped and chromium-doped materials did not change over three months storage of the samples in air.

In HTSC materials, for example $YBa_2Cu_3O_{7-y}$, the ions $Cu^{2+}$ and $Cu^{3+}$ have magnetic moments of 1.9 $\mu_B$ and 3.2 $\mu_B$ respectively. It is necessary to note, that the magnetic moment of $Cr^{3+}$ is 3 $\mu_B$. In relation to this, replacement of copper by chromium on the $Cu^{3+}$ sites can effect a non-significant reduction of the resulting magnetic moment in the product. Results are presented in the Table 2, which indicate that upon replacement of Cu by Cr the bulk magnetic moment of whole the product increases. The $\chi$ temperature dependence is rather significant. For example, in $YBa_2Cu_3O_{7-y}$ at 85 K the $\chi$ value of 64.4 $cm^3/g$ is almost three times the same characteristic at room temperature. It is related to the considerably large ordering in the structures containing magnetic cations, at low temperatures. However, the tendency of reducing $\chi$ with increasing *x* is kept without temperature dependence. So, the $\chi$ value at x = 0.25 and 85 K makes 38.9 ($cm^3/g$).

The same magnitude for the reduction in $T_c$ is also observed for the sample made from reaction of $Y_{123}$ with chromium oxide. These facts together with the increase of X-ray cell parameters values gives evidence that chromium preferentially occupies the $Cu^{3+}$ sites in the HTSC structure due to the similar orbital structure, ionic radii and electron affinity.

### *Modeling experiments in the SHS-systems*

In comparison with previous SHS of $LnBa_2Cu_{3-x}Cr_xO_7$ [17] where copper powder PMS-1 (Russia) (particle size < 60 microns) was used, in this work 10 micron Cu powder was used. The parameters that influence the combustion process are the pressure of oxygen ($PO_2$), green mixture density (d) and the dispersivity of the raw material (especially the copper metal particles size). Over a 20-1000°C range of linear heating a PMS-1 copper powder in air is oxidized giving three exothermic peaks at 270°C, 430°C and 490°C in the DTA. This may be explained by the significant granulometric heterogeneity of the powder and, as a consequence, various oxidation velocities of the different sized fractions. During oxidation of the Aldrich copper metal powder, due to its much greater uniformity, one wide oxidation peak is seen at

200-700°C (Fig. 3a). The weight reduction for the initial stage at T ≤ 100°C corresponds to adsorbed water loss ~ $0.5H_2O$. In the temperature range of 250-500°C a weight increase of 11% occurs, which corresponds to the reaction $2Cu + 0.5O_2 \rightarrow Cu_2O$. A further weight increase (up to ~ 26%) was observed to 500°C when the oxidation of Cu(I) → Cu(II) oxide was promoted. An exothermic peak with a maximum at 550°C on the DTA cooling curve also corresponds to the end of this reaction. The incompleteness of the oxidation of Cu metal is related to the formation of oxide layers limiting diffusion.

The presence of 5% chromium (III) oxide in the copper metal charge changes the temperature of maximum heat release in the oxidation from 300 to 313°C, and the exothermic peak is less defined (Fig. 3b). The intensity of heat release is reduced from ~ 80 mV up to ~ 60 mV, and the temperature range of intensive oxidation was also altered. However, as a result of "heating up to 1000°C + cooling down to $T_{room}$" the process of copper oxidation to CuO was also practically finished. This was confirmed by the increase of the samples weight to ~ 23%. It is also necessary to note, that during heating this mixture not only does copper oxidation take place, but also some formation of $CuCr_2O_4$. One of the peaks on a DTA curve (at higher temperature) is connected with the copper chromite crystallization, and the second peak at lower temperatures - copper oxidation to CuO.

Barium peroxide $BaO_2$ decomposition occurs at 650-900°C with maximum heat release at 855°C (Fig. 3c). Its oxygen desorption rate essentially increases with temperature. The weight loss in the decomposition reaction makes ~ 8.7%, that corresponds to the reaction $BaO_2 \rightarrow BaO + 0.5O_2$ [15]. Figure 2c shows TGA and DTA curves of barium carbonate ($BaCO_3$) - the source of barium in most conventional HTSC preparations. An endothermic effect at T ~ 370-400°C on the DTA curve is related to the eutectics of $BaCO_3$ - $Ba(OH)_2$ melting. Pure industrial $BaO_2$ contains ~ 93-95% of the basic substance. The occurrence of eutectics is caused by melting of $Ba(OH)_2$ ~ 1-2% and $BaCO_3$ ~ 3-5% impurities. Polymorph endothermic transitions take place in the structure of $BaCO_3$ with increasing temperature. The first endothermic peak on a DTA curve, appropriate to polymorph transition of $BaCO_3$ from rhombic to hexagonal occurs at T = 820°C. A second - from hexagonal to cubic, takes place at T = 950°C. These transitions are accompanied by partial loss of $CO_2$ ~ 4% from barium carbonate.

In the mixture of $2BaO_2 + 2.8Cu + 0.1Cr_2O_3$ (Fig. 3d) up to T ~ 350°C copper does not undergo oxidation. At 313°C, in this system, the oxidizing reaction of chromium (III) oxide proceeds at the expense of partial decomposition of $BaO_2$: $BaO_2 \rightarrow BaO + 0.5O_2$

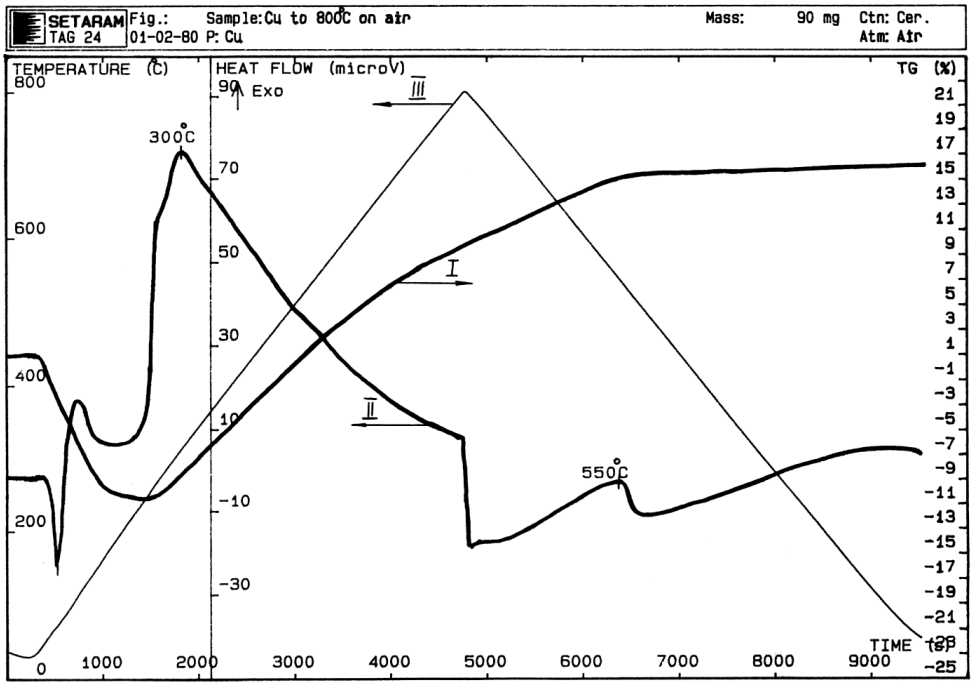


Fig. 3a. TGA (I), DTA (II) and temperature (III) curves for the copper (Aldrich [32,645-3] (UK)) metal powder oxidation processes under linear heating.

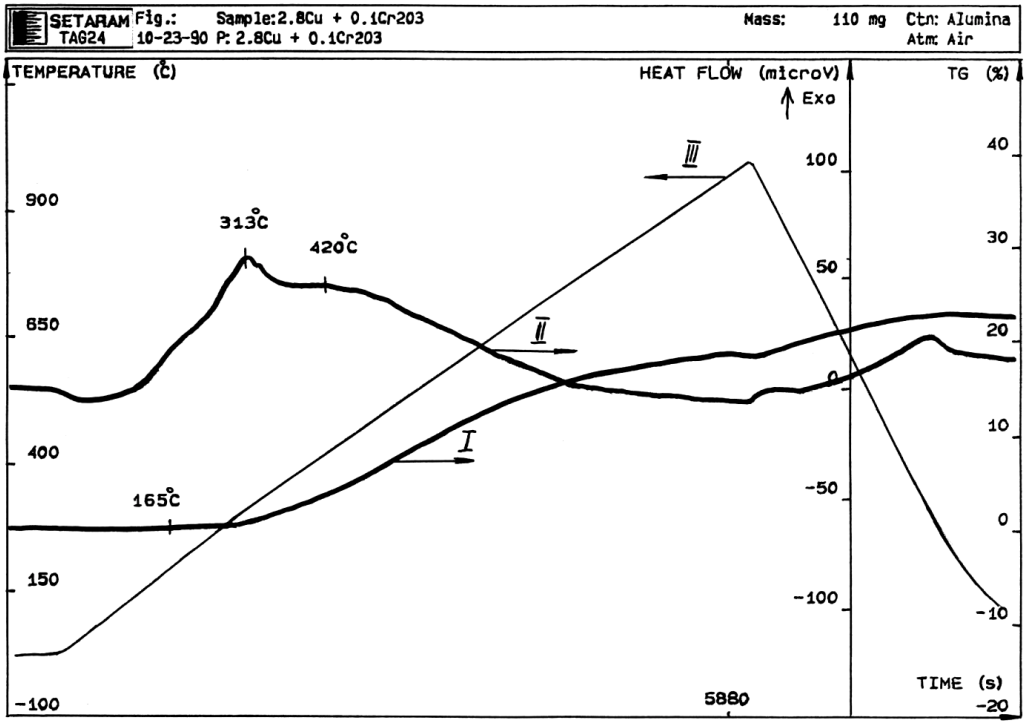


Fig. 3b. TGA (I) and DTA (II) and temperature (III) curves for the reaction 2.8Cu + 0.1$Cr_2O_3$ under linear heating.

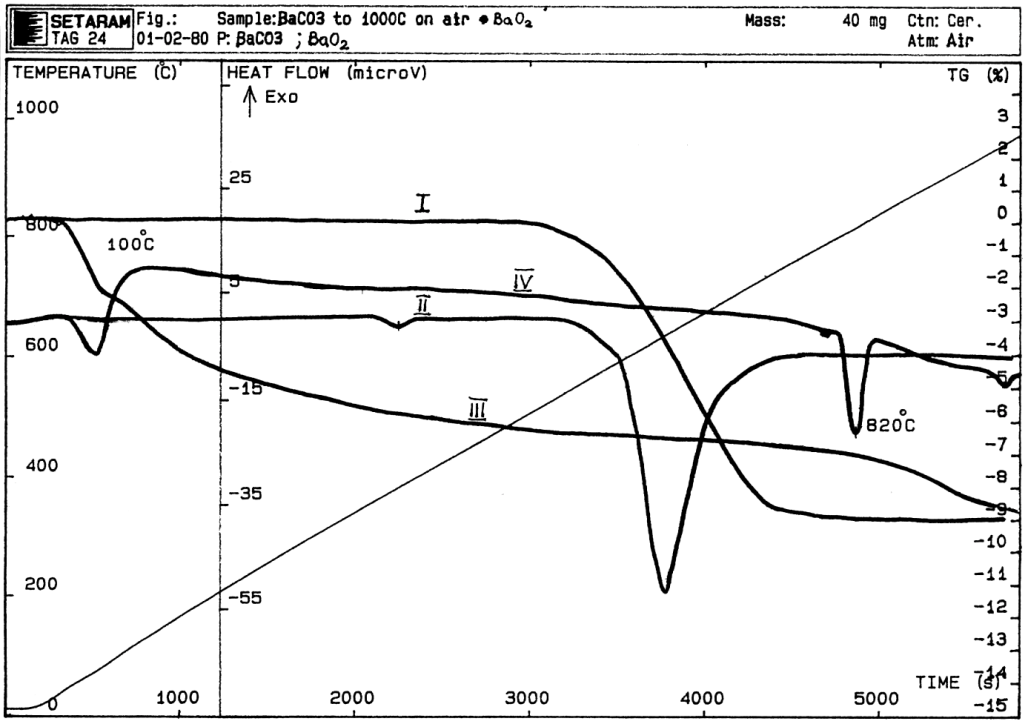


Fig. 3c. TGA (I) - DTA (II) curves for the $BaO_2$ (under argon atmosphere) and TGA (III) – DTA (IV) curves for $BaCO_3$ (under air) decomposition under conditions of linear heating.

and liquid phase formation. The liquid phase influences the process of copper oxidation at T > 450°C, and the intensive process of oxidation with maximum at T = 435°C takes place at the expense of the copper interaction with air. With increasing temperature and an increase of the barium peroxide decomposition rate, the limiting stage in the process becomes that of copper oxidation, which proceed up to temperatures ~ 700°C

and has a maximum at T = 650°C. Over this temperature range there is also a partial formation of copper chromite. The general weight increasing in the system is 4.5%. At 925°C barium cuprate $BaCuO_2$ melting occurs, which leads to the eutectics in the copper chromite $CuCr_2O_4$ formation. On cooling, the DTA curve shows the peak for the barium cuprate $BaCuO_2$ crystallization process at T = 800°C.

The interaction of the components in the $0.5Y_2O_3 + 2.8Cu + 0.1Cr_2O_3$ mixture (Fig. 3e) has insignificant differences from the process of copper oxidation in air (TGA curve) and the process of linear heating of the $2.8Cu + 0.1Cr_2O_3$ mixture (curve DTA). The temperatures of the DTA curve peak maxima are higher by some tens of degrees, than in case where yttrium oxide was absent. Finely dispersed powder (< 5 microns) such as $Y_2O_3$ discourages oxygen diffusion through the layers of the homogeneous mixture. The oxide film formation on the copper particles during heating is only partially completed. The exothermic peak seen in the DTA curve during copper oxidation is related to that observed on cooling. The maximum of heat release in this process evolve ~ 50 mV, that is lower than heat release in the system of $2.8Cu + 0.1Cr_2O_3$ which is ~ 60 mV. It is necessary to note, that in previous reports [18] the interaction of yttrium oxide with copper (II) oxide and formation of $Y_2Cu_2O_5$ has a solid-phase nature and was not accompanied by any thermal effects in the DTA curve.

In general, the phase formation mechanism of the chromium-substituted HTSC synthesis differs slightly from the mechanism in non doped systems (Fig. 4). Owing to the fast heating of a mixture in the combustion wave, part of the copper particles (as a rule the larger fractions), have no time to oxidize to the melting state. Copper oxidation process take place in two directions: directly by oxygen from the air through the formation of friable $Cu_2O \cdot CuO$, or through the interaction with oxygen released from $BaO_2$ to form $BaCuO_2$ or $BaCu_2O_2$. Further, the formation of a mixed melt of barium cuprates with copper (II) oxide - $BaCuO_2$- $BaCu_2O_2$- CuO takes place. In the case of chromium (III) oxide $Cr_2O_3$ or chromium (VI) oxide $CrO_3$ as a Cr source a general decrease in the eutectic melt formation occurs owing to the partial change of energy on melting and decomposing (in a case of $CrO_3$) of these compounds. The oxygen deficit in an initial mixture during the combustion process in air can be partially compensated by $CrO_3$ decomposition at T ~ 200°C. Together with chromium-containing solid-oxidizer as an internal source of oxygen, alkaline and alkaline-earth metals perchlorates

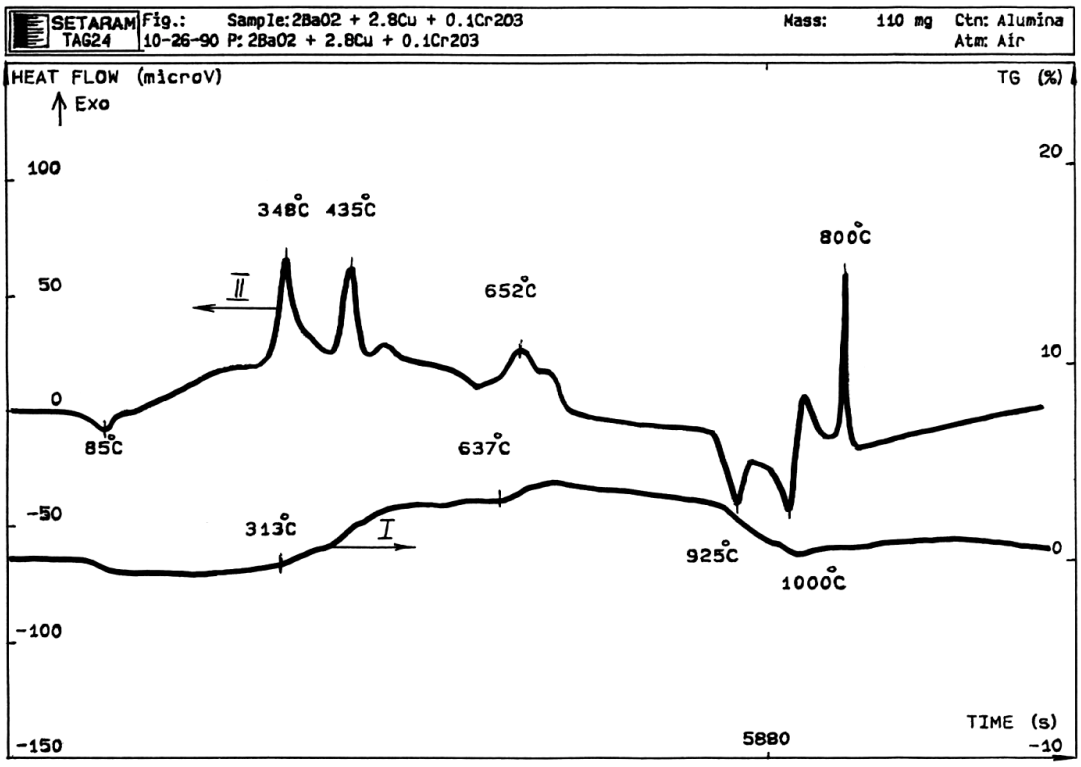


Fig. 3d. TGA (I) and DTA (II) curves for the reaction $2BaO_2 + 2.8Cu + 0.1Cr_2O_3$ under linear heating.

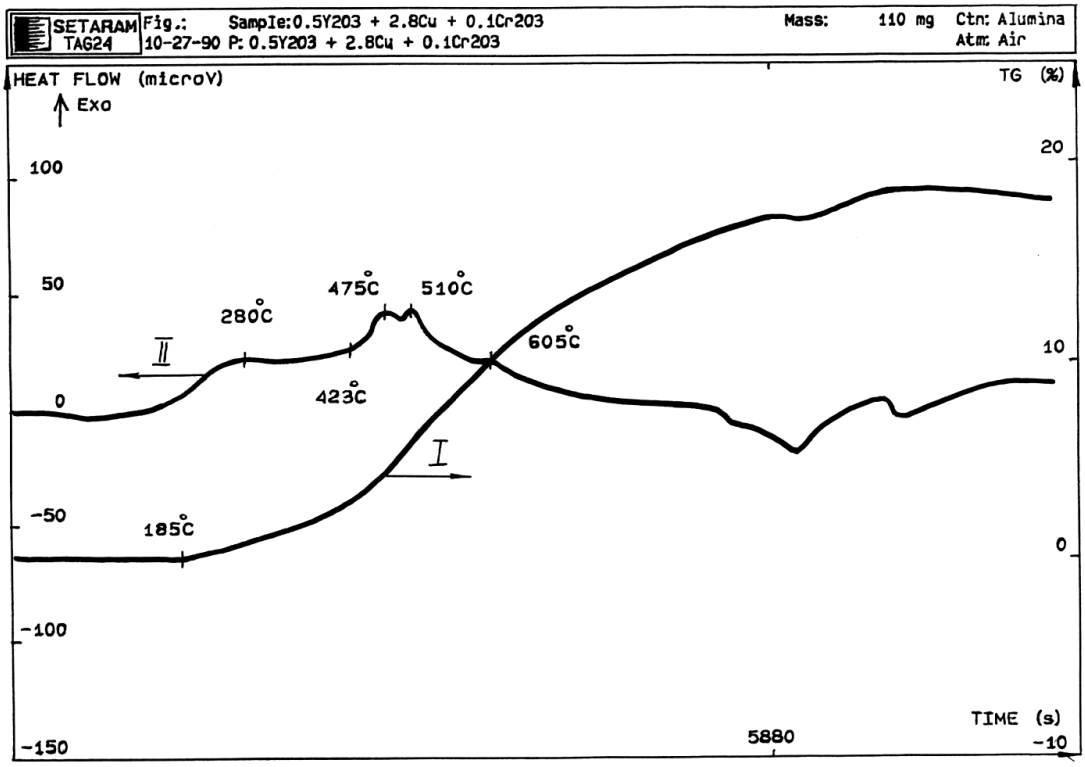


Fig. 3e. TGA (I) and DTA (II) curves for the reaction $0.5Y_2O_3 + 2.8Cu + 0.1Cr_2O_3$ under linear heating.

can also be used for compensation of the oxygen deficiency in the starting materials by decomposition at relatively low temperatures. In each particular scheme of synthesis the perchlorate and chromium (VI) oxide amount was calculated with respect to the oxygen balance (7-y = 7.0) between the initial components and final HTSC product. Analysis of the combustion products in the mixture of $2BaO_2 + 3Cu$ has shown, that together with barium cuprate, copper (II) oxide (~ 5%) was present. In the presence of chromium oxide, the reaction of $BaCuO_2 + CuO \rightarrow BaCu_2O_2 + 0.5O_2$ is not complete, and there is a partial interaction between CuO and $Cr_2O_3$ to form $CuCr_2O_4$ during the initial reaction stage. It is known, that copper chromite is thermally unstable at T ~ 900°C [19] and, hence, its formation proceeds at lower temperatures. At 820-900°C the complex structure melt: $xBaCuO_2$-$yBaCu_2O_2$-$CuCr_2O_4$ was formed. The «y» value depends on the percentage $Cr_2O_3$ and decreases with chromium contents in the system (x + y = 2). During the stage of intermediate product formation, analysis of quenched samples reveals that the chromium (III) oxide is present. In this connection it is possible to make a conclusion that the chromium has reacted via chromium (III) oxide and copper oxide and in the melt of cuprates is present only as $CuCr_2O_4$. In the mixed cuprate melt $Y_2O_3$ was also dissolved with the subsequent crystallization of Cr-doped HTSC phase of $Y_{123}$.

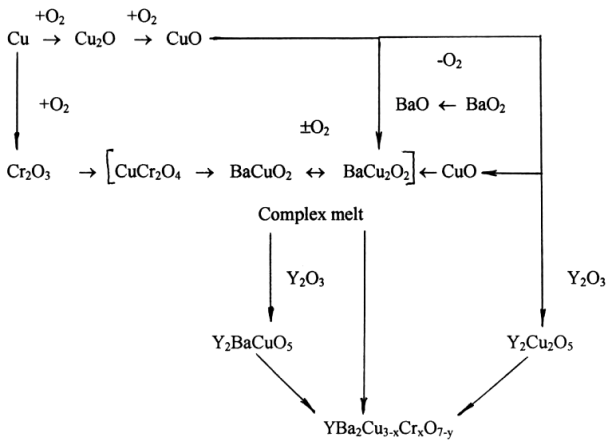


Fig. 4. General scheme of $LnBa_2Cu_{3-x}Cr_xO_{7-y}$ (Ln = Y) preparation by SHS.

HTSC materials were easier to form by SHS with lanthanides of smaller ionic radii. This tendency was especially true for the reactions that has a low exothermic and consequently employed a solid-oxidizer. The maximum combustion temperatures in all the SHS reactions to form $Ln_{123}$ are 890-930°C. All the SHS products have $T_c$ in the range of 77-98 K. It is necessary to emphasize, that the combustion temperature $T_{comb}$ generated in the SHS-processes is similar

to the temperature in the standard ceramics synthesis of $Ln_{123}$ - about 950°C. However, the duration of furnace heating in conventional synthesis is two orders of magnitude longer, than SHS. This long duration is requiring in standard ceramics synthesis as metals oxides are used. In SHS the complex oxides formation occurs simultaneously with oxidation of one of the components – the Cu fuel. From this point of view the SHS route has a more active stage in the chemical reaction.

## Conclusions

Pure and chromium-substituted complex oxides $LnBa_2Cu_{3-x}Cr_xO_{7-y}$ (x = 0-0.25; Ln = Y or REM) were synthesized by self-propagating high-temperature synthesis. All the reactions after sintering at 950°C in an oxygen atmosphere produced single phase orthorhombic or tetragonal $LnBa_2Cu_{3-x}Cr_xO_{7-y}$ with $T_c$ = 98-77 K. The SHS prepared $LnBa_2Cu_{3-x}Cr_xO_{7-y}$ show uniform changes in the $T_c$, lattice parameters, unit cell volumes and magnetic properties ($\chi$) with chromium content and lanthanide atomic number. The SHS materials are equal in quality and characteristics to traditionally prepared materials and require relatively simple synthesis conditions.

## Acknowledgements

Dr. M. V. Kuznetsov thanks the Royal Society of Chemistry, INTAS (YSF) and Russian "Science Support Foundation Grant for Talented Young Researchers" that facilitated this work.

## References

1. Xiao G., Streitz F. H. and Gavrin A., Phys. Rev. B., 35:8782 (1987)
2. Ponomarev V. I., Peresada A. G., Nersesyan M. D. and Merzhanov A. G., Superconductivity: physics, chemistry, technics, 3:2813 (1990)
3. Kuznetsov M. V., Peresada A. G., Morozov Yu. G., Nersesyan M. D. and Ponomarev V. I., Inorg.Mater., 30:89 (1994)
4. Den T. and Cobayashi T., Physica C, 196:141 (1992)
5. Andresen P. H., Fjellvag H., Karen P. and Kjekshus A., Acta Chemica Scandinavica, 45: 698 (1991)
6. Miura N., Suzuta H., Teraoka Y. and Yamazoe N., Jap.J.Appl.Phys., 27:L337 (1988)
7. Khainovskii N. G., Pavlyukhin Y. T. and Boldyrev V. V., Inorg.Mater., 28:648 (1992)
8. Abrikosov A. A. and Gorkov I. P., Phys.Rev.B, 49:12337 (1994)
9. Merzhanov A. G., Borovinskaya I. P., Nersesyan M. D., Peresada A. G. and Morozov Yu. G., Dokladi Akademii Nauk SSSR, 311:96 (1990)
10. Umardevi Muralindharan P., Phys. Status Solidi A, 123:K39 (1991)
11. Umardevi Muralindharan P. and Ramamohan T. R., Phys. Status Solidi A, 130:153 (1992)
12. Umardevi Muralindharan P. and Damodaran A. D., Jap.J.Appl.Phys., 30:280 (1991)
13. Kasperczyk J., Piasecki M. and Bak Z., Physica C, 153-155:215 (1988)
14. Huber J. G., Liverman W. J. and Xu Y., Phys. Rev. B, 41:8757 (1990)
15. Strobel P., Paulsen C. and Tholence J. L., Sol.St.Comm., 65:585 (1988)
16. Semenovskaya S., Zhy Y. and Suenaga M., Phys. Rev B, 47:12182 (1993)
17. Peregudov A. N., Peresada A. G., Karpov L.G. and Peregudova T. V., Chem.Phys.Repts, 11:289 (1992)
18. Lebrat J.P. and Varma A., Combust. Sci. Technol., 88:177 (1993)
19. Kale G. M., J.Mater.Sci., 30:1420 (1995)

*Received 12 January 2002.*